



ARTICLE

CCL5 deficiency promotes liver repair by improving inflammation resolution and liver regeneration through M2 macrophage polarization

Meng Li¹, Xuehua Sun², Jie Zhao¹, Lei Xia¹, Jichang Li¹, Min Xu¹, Bingrui Wang¹, Han Guo¹, Chang Yu¹, Yueqiu Gao², Hailong Wu³, Xiaoni Kong^{1,2} and Qiang Xia¹

Despite the diverse etiologies of drug-induced liver injury (DILI), innate immunity activation is a common feature involved in DILI progression. However, the involvement of innate immunity regulation in inflammation resolution and liver regeneration in DILI remains obscure. Herein, we identified the chemokine CCL5 as a central mediator of innate immunity regulation in the pathogenesis of DILI. First, we showed that serum and hepatic CCL5 levels are elevated in both DILI patients and an APAP-induced liver injury (AILI) mouse model. Interestingly, both nonparenchymal cells and stressed hepatocytes are cell sources of CCL5 induction in response to liver injury. Functional experiments showed that CCL5 deficiency has no effect on the early phase of AILI but promotes liver repair in the late phase mainly by promoting inflammation resolution and liver regeneration, which are associated with an increased number of hepatic M2 macrophages. Mechanistically, CCL5 can directly activate M1 polarization and impede M2 polarization through the CCR1- and CCR5-mediated activation of the MAPK and NF- κ B pathways. We then showed that CCL5 inhibition mediated by either a CCL5-neutralizing antibody or the antagonist Met-CCL5 can greatly alleviate liver injury and improve survival in an AILI mouse model. Our data demonstrate CCL5 induction during DILI, identify CCL5 as a novel innate immunity regulator in macrophage polarization, and suggest that CCL5 blockage is a promising therapeutic strategy for the treatment of DILI.

Keywords: CCL5; APAP; macrophage polarization; acute liver injury

Cellular & Molecular Immunology (2020) 17:753–764; <https://doi.org/10.1038/s41423-019-0279-0>

INTRODUCTION

Drug-induced liver injury (DILI), particularly acetaminophen (APAP)-induced liver injury (AILI), is the most common cause of acute liver failure (ALF) in the West.¹ AILI sequentially includes three pathologic phases: injury initiation, injury amplification, and liver regeneration and repair.² Once APAP is ingested, overdosed APAP can be catalyzed by CYP2E1 to form a reactive metabolite, *N*-acetyl-*p*-benzoquinone imine (NAPQI), which causes glutathione (GSH) depletion and mitochondrial dysfunction, to initiate injury.^{2,3} Then dysfunctional mitochondria lead to cellular ATP depletion, DNA fragmentation, cell necrosis, and the activation of resident liver macrophages (Kupffer cells (KCs)) to further amplify the injury.^{2,4} Finally, cytokines and chemokines secreted by activated KCs further attract the homing and transmigration of neutrophils and macrophages to facilitate hepatic inflammation resolution, regeneration, and repair. Currently, *N*-acetyl cysteine (NAC), a precursor of GSH, is the only approved treatment for AILI.⁵ Because NAC works mainly by detoxifying NAPQI,⁶ NAC treatment is only effective for 8 h after the ingestion of APAP and is less effective in late-presenting

patients.⁷ Therefore, the development of alternative approaches or targets for the late stages of APAP overdose is urgently required.

Macrophages have been reported to play a dichotomous role in regulating both tissue-destructive and resolution/repair events in AILI. For example, on the one hand, macrophages aggravate inflammation through IL-1 α -mediated chemoattraction and the activation of CD11b⁺Gr-1⁺ myeloid cells during AILI^{8,9}; on the other hand, they can also promote inflammation resolution and injury repair by removing necrotic cell debris.² These controversial roles of hepatic macrophages in AILI are mainly attributed to their inherent plasticity caused by the polarization of macrophages toward M1 (pro-inflammatory) or M2 (anti-inflammatory) phenotypes in response to various stimuli.^{10,11} Generally, M1 macrophages damage contiguous tissues and inhibit the proliferation of surrounding cells by producing proinflammatory cytokines and chemokines to trigger intracellular cell death mechanisms,² whereas M2 macrophages promote inflammation resolution, contiguous tissue repair, and cell proliferation by releasing anti-inflammatory cytokines such as IL-10 and by cleaning up necrotic

¹Department of Liver Surgery, Renji Hospital, School of Medicine, Shanghai Jiao Tong University, Shanghai, China; ²Institute of Clinical Immunology, Department of Liver Diseases, Central Laboratory, Shugang Hospital Affiliated to Shanghai University of Chinese Traditional Medicine, Shanghai, China and ³Shanghai Key Laboratory of Molecular Imaging, Collaborative Research Center, Shanghai University of Medicine & Health Science, Shanghai, China

Correspondence: Hailong Wu (wuhailong2@163.com) or Xiaoni Kong (xiaoni-kong@126.com) or Qiang Xia (xiaqiang@shsmu.edu.cn)

These authors contributed equally: Meng Li, Xuehua Sun, Jie Zhao

Received: 7 August 2019 Accepted: 11 August 2019

Published online: 3 September 2019

cell debris.^{2,12} Therefore, the extent of hepatic inflammation and repair is largely determined by the balance between M1 and M2 polarization, and strategies targeting macrophage polarization may be an effective means of alleviating acute liver injury and benefiting ALF patients.

C-C chemokine motif ligand 5 (CCL5), also known as RANTES, functions as a professional chemoattractant that directs the migration of leukocytes into inflammatory lesions in various pathological processes.¹³ It has been reported that CCL5 performs its biological functions by activating downstream signaling pathways such as the signal transducer and activator of transcription factor 3, nuclear factor (NF)- κ B, and mitogen-activated protein kinase (MAPK) pathways through three cell surface receptors, namely, C-C chemokine motif receptor 1 (CCR1), CCR3, and CCR5.^{14–16} CCL5 can be produced in many cell types, including platelets, macrophages, eosinophils, fibroblasts, endothelium, epithelial, and endometrial cells, suggesting that CCL5 plays diverse roles in many physiological and pathological processes.¹⁷ In fact, previous studies have demonstrated the implications of CCL5 in various liver diseases, including fibrosis, non-alcoholic fatty liver disease (NAFLD), cirrhosis, and hepatocellular carcinoma (HCC).¹⁷ For example, CCL5 has been identified as a pivotal regulator essential for early fibrogenic events during NAFLD development, and the antagonization of CCL5 by Met-CCL5, an antagonist of CCR1 and CCR5, significantly alleviates experimental hepatic fibrosis in mice^{18,19}; in cirrhotic patients, high serum levels of CCL5 may indicate the presence of HCC,²⁰ and inhibiting CCL5 in vivo seems to be an encouraging approach for patients with liver cirrhosis.²¹ In addition, CCL5 has been reported to aggravate liver ischemia/reperfusion (IR) injury by chemoattracting macrophages.²² However, the role of CCL5 in AILI remains unclear.

Here we show a significant increase in CCL5 in both DILI patients and an AILI mouse model. Functional studies indicate that the genetic loss of *Ccl5* promotes liver repair by improving inflammation resolution and liver regeneration associated with enhanced M2 polarization of macrophages in the AILI mouse model. Mechanistically, we demonstrate that CCL5 directly facilitates M1 polarization and impedes M2 polarization through the CCL5-CCR1- and CCL5-CCR5-mediated activation of the MAPK and NF- κ B pathways. Finally, we indicate that CCL5 inhibition may serve as a promising therapeutic strategy for APAP overdose and suggest its possible application in other acute liver injuries induced by carbon tetrachloride (CCl₄) or IR.

RESULTS

Upregulation of CCL5 in DILI patients and an AILI mouse model
To examine the role of CCL5 in DILI, we first examined CCL5 levels in DILI patients. In a cohort of 15 DILI patients, serum CCL5 levels were significantly increased compared with those in healthy controls ($n = 15$; Fig. 1a), especially in APAP-induced liver injury (Supplementary Table 1). In addition, hepatic CCL5 levels were also evaluated by immunohistochemical (IHC) staining in DILI patients. As shown in Fig. 1b, hepatic CCL5 levels were greatly increased in DILI patients compared to healthy controls. According to the morphological observations of hepatic CCL5-positive cells, we found that CCL5 was expressed in both nonparenchymal cells (NPCs) and hepatocytes in DILI patients (Fig. 1b). To further confirm the elevation of CCL5 levels in DILI, we examined CCL5 levels in an APAP-induced liver injury mouse model.²³ Consistent with the changes in CCL5 levels in DILI patients, APAP administration induced a marked increase in CCL5 levels in both the serum and liver tissues (Fig. 1c, d). IHC also showed CCL5 induction in NPCs and hepatocytes after APAP challenge compared with that in normal controls (Fig. 1d). To further identify the cell source of CCL5, we examined *Ccl5* mRNA levels in both hepatocytes and

NPCs from the liver of mice post-APAP challenge by quantitative polymerase chain reaction (qPCR). Compared to that in normal controls, *Ccl5* transcription was greatly induced in both hepatocytes and NPCs after APAP treatment (Fig. 1e), suggesting that multiple types of cells contribute to CCL5 elevation in AILI. These findings indicate that CCL5 is induced in both DILI patients and an AILI mouse model.

CCL5 deficiency induces rapid liver recovery in the late phase of APAP treatment

To investigate the biological role of CCL5 in DILI, we established an APAP-induced liver injury mouse model (300 mg/kg APAP, intraperitoneal (i.p.)) in both wild-type (WT) and *Ccl5*^{-/-} mice. Although both genotypes displayed comparable liver injury 24 h after APAP treatment, *Ccl5*^{-/-} mice showed rapid liver recovery in the late phase after APAP challenge, as evidenced by significantly decreased alanine aminotransferase (ALT)/aspartate aminotransferase (AST) induction (Fig. 2a) and hepatic necrosis (Fig. 2b) 36–48 h after APAP treatment. Consistently, terminal deoxynucleotidyl transferase-mediated dUTP-fluorescein nick end labeling assays also demonstrated fewer hepatic necrosis in *Ccl5*^{-/-} mice in the late phase after APAP challenge (Fig. 2c). Corresponding to the prorecovery role of CCL5 deficiency in the AILI model, survival assays in the APAP-induced ALF mouse model (500 mg/kg APAP, i.p.) showed significantly improved survival in *Ccl5*^{-/-} mice compared to WT mice (Fig. 2d). Given that CCL5 deficiency causes enhanced liver recovery in the late phase after APAP challenge, it is very unlikely that early detrimental events such as APAP metabolism or mitochondrial dysfunction are involved in such a protective effect. As expected, hepatic GSH and CYP2E1 protein levels were comparable 2 and 6 h after APAP treatment in both genotypes (Fig. S1A, B). In addition, the measurement of the mitochondrial membrane potential $\Delta\Psi$ m (using JC-1 fluorescent dye) further confirmed that CCL5 deficiency had no effect on APAP-induced mitochondrial dysfunction (Fig. S1C, D). These findings indicate that CCL5 deficiency plays a protective role in the late phase of AILI and suggest that CCL5 may serve as a therapeutic candidate targeting the late stage of APAP-induced ALF.

CCL5 deficiency promotes inflammation resolution and liver regeneration in the late phase of APAP treatment

Given that an acute inflammatory response (mainly 12–24 h after APAP) is a detrimental hallmark of APAP-induced liver injury² and that enhanced inflammation resolution can greatly protect against APAP-induced hepatotoxicity,²⁴ we examined whether the enhanced liver recovery in *Ccl5*^{-/-} mice can be attributed to resolution enhancement. Enzyme-linked immunosorbent assay (ELISA) showed significantly reduced serum tumor necrosis factor- α (TNF α) and interleukin (IL)-6 levels in *Ccl5*^{-/-} mice compared to WT mice 36 and 48 h after APAP treatment (Fig. 3a). By using a well-designed gating strategy (Fig. S2A), we performed flow cytometric assays and found a markedly decreased number of hepatic neutrophils (CD11b⁺Ly6G⁺) in *Ccl5*^{-/-} mice in the late phase after APAP treatment (Fig. 3b). In addition, IHC for Ly6G also confirmed the reduced number of neutrophils in the liver of *Ccl5*^{-/-} mice (Fig. 3c). In addition to inflammatory resolution, hepatocyte regeneration is also critical for liver repair and recovery in ALF patients.^{25,26} Here we also examined hepatocyte regeneration in both genotypes after APAP treatment. Interestingly, we found that Ki67-positive hepatocytes and hepatic proliferating cell nuclear antigen protein levels were significantly increased in *Ccl5*^{-/-} mice compared to WT mice between 36 and 48 h after APAP treatment (Fig. 3d, e). Together, these data suggest that the enhanced liver repair in *Ccl5*^{-/-} mice is associated with improved inflammation resolution and liver regeneration in *Ccl5*^{-/-} mice after APAP treatment.

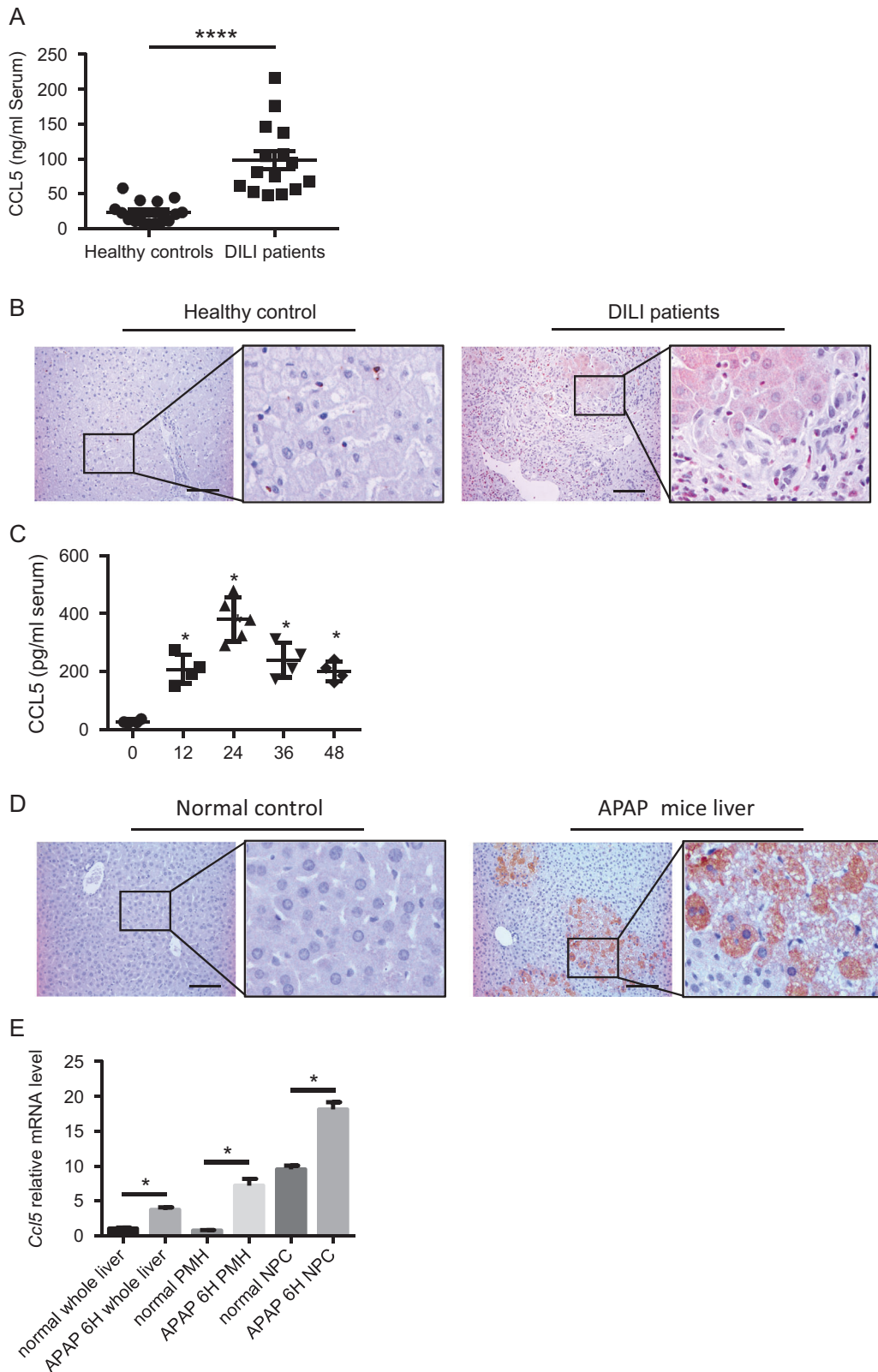


Fig. 1 CCL5 induction in DILI patients and an ALLI mouse model. **a** ELISA analysis of serum CCL5 levels in DILI patients ($n = 15$) and healthy controls ($n = 15$). **b** Representative IHC images of hepatic CCL5 expression in DILI patients and healthy controls (original magnification = $\times 200$, scale bar = $100 \mu\text{m}$). **c** Dynamic serum CCL5 levels in WT mice after APAP challenge at the indicated time points ($n = 4-6$). **d** Representative IHC images of hepatic CCL5 expression in WT mice 24 h after APAP treatment and in normal controls (original magnification = $\times 200$, scale bar = $100 \mu\text{m}$). **e** Relative *Ccl5* mRNA expression was determined in liver tissues, primary hepatocytes (PMHs), and nonparenchymal cells (NPCs) 6 h after APAP treatment ($n = 3-4$). The data are shown as means \pm SEM, $*P < 0.05$, $****P < 0.0001$

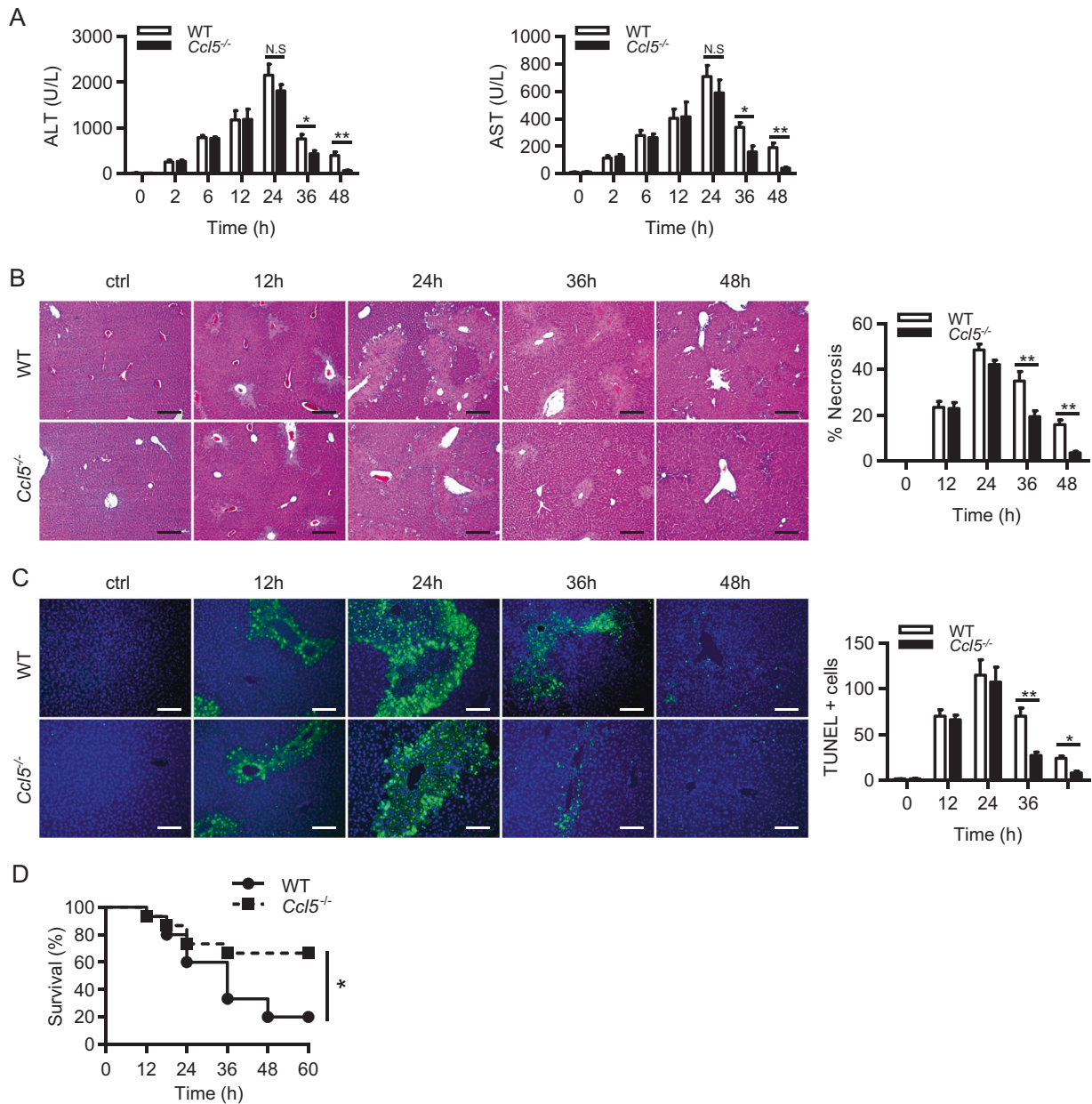


Fig. 2 *Ccl5*^{-/-} mice display rapid liver recovery after APAP treatment. **a–c** APAP treatment in both *Ccl5*^{-/-} and WT mice at the indicated time points (*n* = 4–6). **a** Serum levels of ALT/AST of both genotypes. **b** Representative images of H&E staining (original magnification = ×100, scale bar = 200 μm) and the statistical quantification of hepatic necrosis. **c** Representative images of TUNEL staining (original magnification = ×200, scale bar = 100 μm) and the statistical quantification of TUNEL-positive cells. **d** Survival curve of *Ccl5*^{-/-} and WT mice in response to a lethal dose of APAP (*n* = 15). The data are shown as means ± SEM, **P* < 0.05, ***P* < 0.01

CCL5 deficiency improves liver repair by enhancing M2 macrophage polarization

Given that CCL5 is a chemokine that recruits many types of leukocytes, we then performed a flow cytometric assay to determine whether there are differences in the hepatic infiltration of leukocytes in the two genotypes. As shown in Fig. 4a and Fig. S2B, the numbers of hepatic monocyte-derived macrophages (CD11b^{high}F4/80^{int}), KCs (CD11b^{int}F4/80^{high}), and natural killer (NK) (NK1.1^{high}CD3⁻), NKT (NK1.1^{int}CD3^{int}), B (CD19⁺CD3⁻), CD8⁺ T (CD3⁺CD8⁺), and CD4⁺ T (CD3⁺CD4⁺) cells were comparable in both genotypes in the late phase after APAP treatment. Among macrophages, M2 macrophages have been proven to play a potent role in inflammation resolution and the phagocytosis of cell debris.^{2,27} We then examined the population of M2

macrophages in both genotypes. By analyzing the levels of CD206 (a surface marker of M2 macrophages)²⁸ by flow cytometry, we demonstrated a higher number of hepatic M2 in *Ccl5*^{-/-} mice than in WT mice 36 h after APAP treatment (Fig. 4b), suggesting that the increase in the number of M2 macrophages may contribute to resolution enhancement in *Ccl5*^{-/-} mice. Moreover, the increased number of M2 macrophages in *Ccl5*^{-/-} mice was further confirmed by detecting the levels of M1 markers (inducible nitric oxide synthase, TNFα, IL-1β) and M2 markers (Arg1, Ym1, CD206) by qPCR (Fig. 4c) and by immunofluorescence costaining for CD68 (a general macrophage marker) and Ym1 (Fig. 4d). These findings indicate that the increase in the number of hepatic M2 macrophages may contribute to improving liver resolution/repair in *Ccl5*^{-/-} mice.

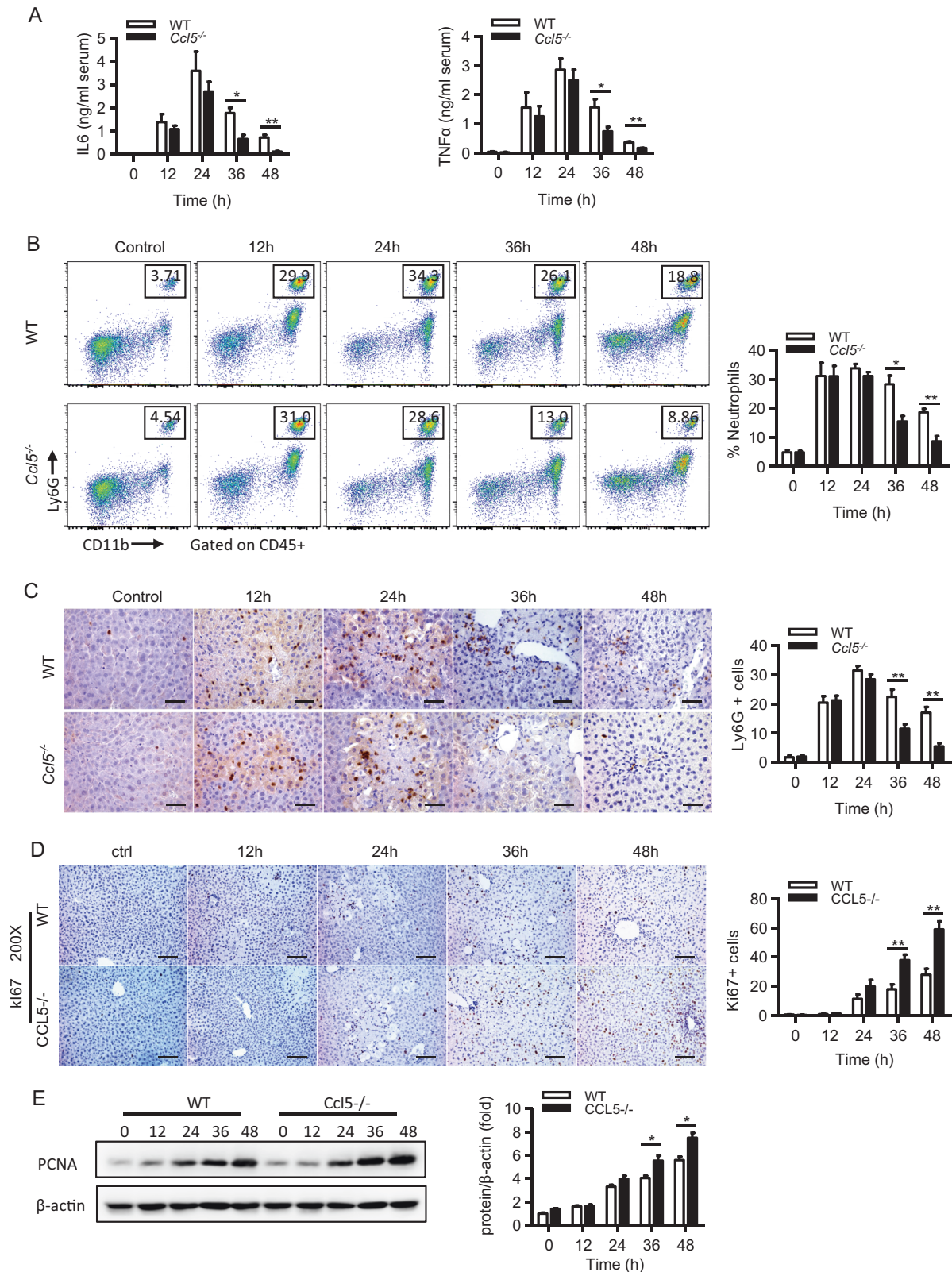


Fig. 3 Enhanced inflammation resolution and liver regeneration in *Ccl5*^{-/-} mice at the late phase of APAP treatment. **a–e** APAP treatment in both *Ccl5*^{-/-} and WT mice at the indicated time points (*n* = 4–6). **a** ELISA analyses of the serum levels of IL-6 and TNFα. **b** Representative FACS plots and the statistical quantification of hepatic neutrophils (Ly6G⁺ CD11b⁺). **c** Representative IHC images and the statistical quantification of hepatic Ly6G⁺ cells in liver sections (original magnification = ×400, scale bar = 50 μm). **d** Representative immunohistochemical staining of hepatic Ki67 in liver sections of *Ccl5*^{-/-} and control mice at the indicated time points after APAP treatment and the quantification of Ki67-positive cells in liver sections (*n* = 4–6). **e** Western blot analysis showing the expression of hepatic PCNA in *Ccl5*^{-/-} and control mice at the indicated time points after APAP treatment and the quantification of hepatic PCNA levels normalized to β-actin (*n* = 3–4). The data are shown as means ± SEM, **P* < 0.05, ***P* < 0.01

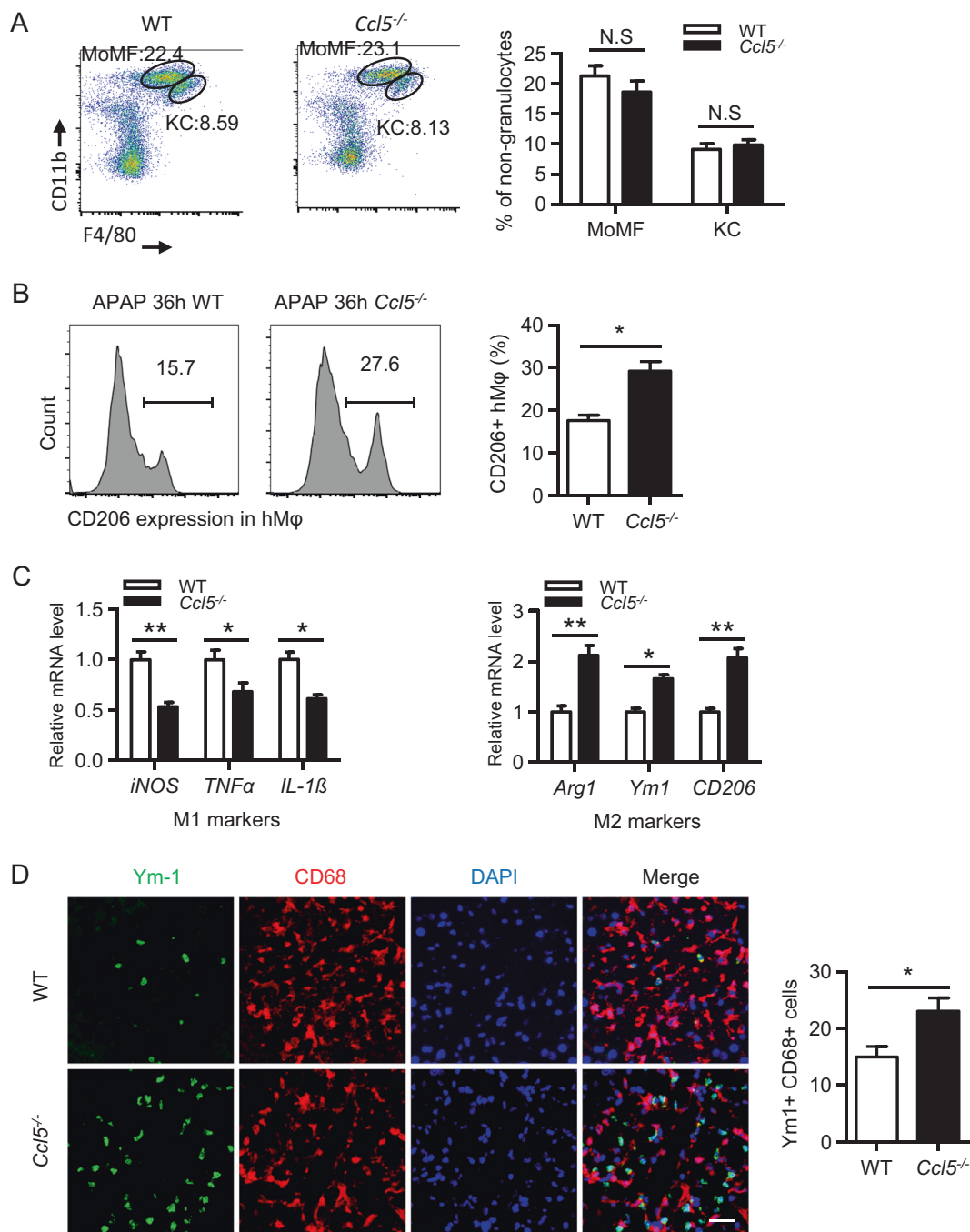


Fig. 4 Increased M2 macrophages in *Ccl5*^{-/-} mice at the late phase of APAP treatment. **a–d** APAP treatment in both *Ccl5*^{-/-} and WT mice at 36 h. **a** Representative MoMF (CD11b^{high}F4/80^{int}) and KC (CD11b^{int}F4/80^{high}) profiles of CD45⁺ liver nongranulocytes from *Ccl5*^{-/-} and WT mice 36 h after APAP treatment and the quantification of the proportion of MoMFs and KCs relative to total CD45⁺ liver nongranulocytes (*n* = 4–6). **b** Representative FACS plots and the statistical quantification of CD206⁺ hepatic macrophages (hMφ) (*n* = 4–6). **c** The relative expression of M1 markers (*iNOS*, *IL-1β*, and *TNFA*) and M2 markers (*Arg1*, *Ym1*, and *CD206*) was determined in FACS-sorted hepatic macrophages (CD45⁺CD11b⁺F4/80⁺) (*n* = 4). **d** Representative images and the statistical quantification of hepatic cells positive for CD68 (a panmacrophage marker) and Ym1 (an M2 macrophage marker) in liver sections (original magnification = ×400, scale bar = 50 μm). The data are shown as the means ± SEM, **P* < 0.05, ***P* < 0.01. hMφ hepatic macrophages

CCL5 directly promotes M1 polarization and impedes M2 polarization in macrophages. Since a significantly increased number of hepatic M2 macrophages was observed in *Ccl5*^{-/-} mice, we then examined whether CCL5 can direct the polarization of macrophages. Polarization assays in peritoneal macrophages (PMφ) and bone marrow-derived macrophages (BMMφ) showed that

recombinant mouse CCL5 (rmCCL5) directly and greatly induced M1 polarization (Fig. 5a, b), and such induction was dose dependent (Fig. S3A). Moreover, rmCCL5-induced M1 polarization was further confirmed in the RAW264.7 macrophage cell line (Fig. S3B). This CCL5-induced M1 polarization is unlikely to be due to contamination of rmCCL5 with endotoxin because rmCCL5 also induced M1 polarization in PMφ isolated from both

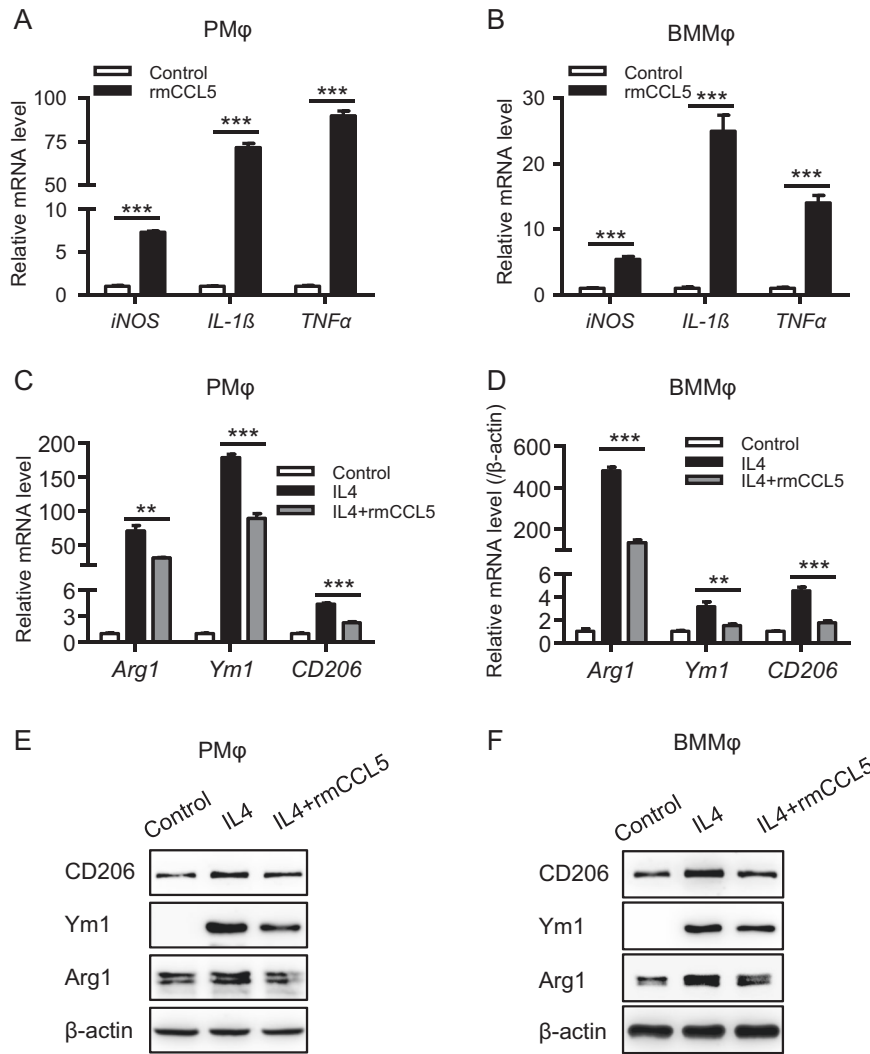


Fig. 5 CCL5 directly regulates macrophage polarization. Mouse peritoneal macrophages (PMφ) and bone marrow-derived macrophages (BMMφ) were stimulated with 100 ng/ml rmCCL5 for 6 h, and the expression of M1 macrophage markers (*iNOS*, *IL-1β*, and *TNFα*) was detected by qPCR in PMφ (a) and BMMφ (b). PMφ and BMMφ were stimulated with 20 ng/ml IL4 and with or without 100 ng/ml rmCCL5 for 6 h, and the expression of M2 macrophage markers (*Arg1*, *Ym1*, and *CD206*) was detected by qPCR in PMφ (c) and BMMφ (d). PMφ and BMMφ were stimulated with 20 ng/ml IL4 and with or without 100 ng/ml rmCCL5 for 24 h, and the expression of M2 macrophage markers (*Arg1*, *Ym1*, and *CD206*) was detected by western blot analysis in PMφ (e) and BMMφ (f). The data are represented as the mean ± SEM of at least three independent experiments. ***P* < 0.01, ****P* < 0.001

WT and *Tlr4*^{-/-} mice, whereas lipopolysaccharide induced M1 polarization in PMφ from WT mice but not from *Tlr4*^{-/-} mice (Fig. S3C). Furthermore, heat inactivation at 100 degrees for 5 min completely abolished rmCCL5-induced M1 polarization in PMφ (Fig. S3D). Interestingly, qPCR assays demonstrated that cotreatment with IL-4 (commonly used to induce M2 polarization) and rmCCL5 significantly impeded IL4-induced M2 polarization in both PMφ and BMMφ (Fig. 5c, d). Moreover, western blot assays further confirmed such CCL5-mediated impairment of M2 polarization (Fig. 5e, f). These findings indicate that CCL5 is a novel polarization regulator that directly induces M1 polarization and impedes M2 polarization, and this explains the greater number of M2 macrophages in *Ccl5*^{-/-} mice during ALLI.

The CCL5-CCR1 and CCL5-CCR5 pathways are required for CCL5-mediated macrophage polarization. Given that the activation of the MAPK and NF-κB signaling pathways is important for M1 polarization,^{29,30} we examined

whether CCL5 can induce the activation of those two pathways. CCL5 treatment greatly activated both the MAPK and NF-κB signaling pathways in PMφ, as indicated by increased protein levels of p-Erk1/2, p-JNK, p-NF-κB, and p-IκBα (Fig. 6a). Moreover, treatment with antagonists of CCR1 (BX471), CCR3 (GW766994), and CCR5 (maraviroc) showed that the CCL5-mediated induction of the MAPK and NF-κB pathways was dependent on CCR1 and CCR5 but not on CCR3 (Fig. 6b). In line with this notion, antagonists blocking CCR1 and CCR5 but not CCR3 significantly impaired CCL5-induced M1 polarization, whereas they markedly enhanced IL4-induced M2 polarization in PMφ (Fig. 6c). Meanwhile, by employing an RNAi-mediated knockdown of CCR1 or CCR5 in RAW264.7 cells, we further confirmed that the inhibition of the CCL5-CCR1 or CCR5 pathway greatly impaired CCL5-induced MAPK and NF-κB activation (Fig. 6d), reduced M1 polarization, and augmented IL4-induced M2 polarization (Fig. 6e). These findings indicate that, through CCR1 and CCR5, CCL5 can activate MAPK and NF-κB pathways, resulting in the enhancement of M1 polarization and the attenuation of M2 polarization in macrophages.

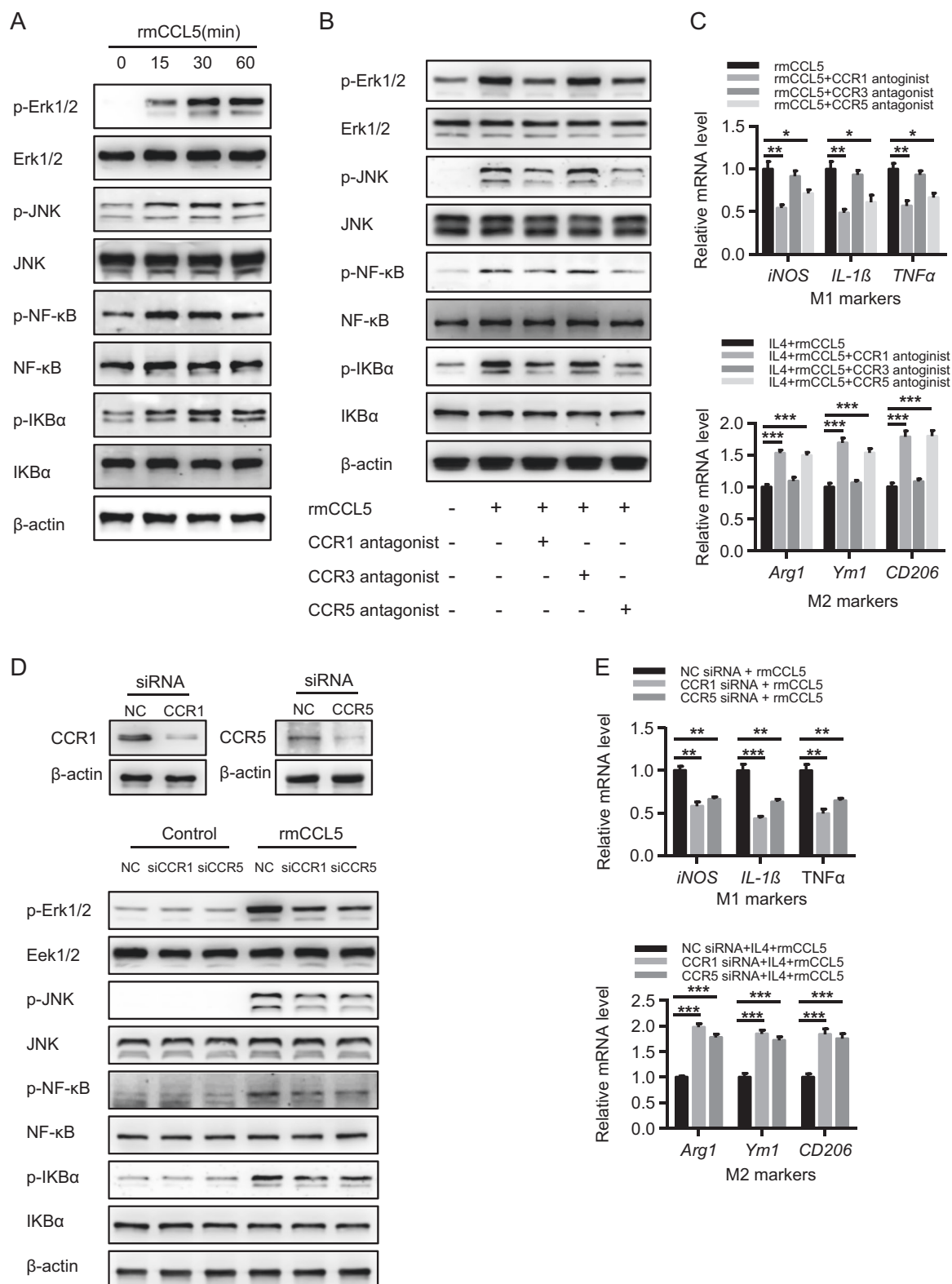


Fig. 6 CCL5 regulates macrophage polarization mainly through CCR1- and CCR5-related MAPK/NF-κB pathways. **a** Mouse peritoneal macrophages (PMφ) were stimulated with 100 ng/ml rmCCL5 for 0–60 min, and the signaling activation of the MAPK and NF-κB pathways was detected by western blot analysis. **b** PMφ were pretreated with a CCR1/3/5 antagonist separately for 1 h and then stimulated with 100 ng/ml rmCCL5 for 30 min. The signaling activation of the MAPK and NF-κB pathways was detected by western blot analysis. **c** PMφ were pretreated with a CCR1/3/5 antagonist separately for 1 h and then stimulated with 100 ng/ml rmCCL5 for 6 h. qPCR analysis of M1 marker and M2 marker expression was performed ($n = 4$). **d, e** Raw 264.7 cells were pretreated with control, CCR1, or CCR5 siRNA separately for 48 h. **d** Western blot analysis detected the knockdown of CCR1 and CCR5. siRNA-treated cells were stimulated with 100 ng/ml rmCCL5 for 30 min, and the signaling activation of the MAPK and NF-κB pathways was detected by western blot analysis. **e** siRNA-treated cells were stimulated with 100 ng/ml rmCCL5 for 6 h, and qPCR analysis of M1 marker and M2 marker expression was performed ($n = 4$). The data are shown as means \pm SEM, * $P < 0.05$, ** $P < 0.01$, *** $P < 0.001$

CCL5 signaling inhibition facilitates liver recovery after acute liver injury

Having detected that CCL5 deficiency improves liver recovery after APAP treatment by enhancing M2 polarization, we then sought to evaluate the therapeutic potential of CCL5 inhibition in APAP-induced liver injury. As shown in Fig. 7a, a CCL5 neutralization antibody (anti-CCL5) or a CCL5 receptor antagonist (Met-CCL5) was administered to WT mice 6 and 24 h after APAP overdose, and liver injury was assessed 36 h after APAP treatment. Both anti-CCL5 and Met-CCL5 greatly promoted APAP-induced liver injury, as demonstrated by significantly decreased ALT/AST levels (Fig. 7b), decreased hepatic necrosis (Fig. 7c), and reduced hepatic neutrophil infiltration (Fig. 7d). In line with the findings in *Ccl5*^{-/-} mice, an increase in the number of hepatic M2 macrophages was also detected in mice treated with anti-CCL5 or Met-CCL5 (Fig. 7e). More importantly, anti-CCL5- or Met-CCL5-mediated CCL5 inhibition greatly improved survival in WT mice following a lethal dose (500 mg/kg, i.p.) of APAP treatment (Fig. 7f). These findings imply the therapeutic potential of targeting CCL5 for the treatment of APAP overdose. Given that M2 macrophages have been reported to promote tissue healing in CCl₄- or IR-induced liver injury,^{31,32} we then tested whether CCL5 signaling inhibition plays protective roles in these liver injury models. As in APAP-induced liver injury, serum CCL5 levels were markedly increased in an acute CCl₄-induced liver injury model (Fig. S4A) and a liver IR model (Fig. S4B). Moreover, CCL5 deficiency improved liver recovery (Fig. S4C, D) while also increasing the hepatic accumulation of M2 macrophages (Fig. S4E) and decreasing the hepatic infiltration of neutrophils (Fig. S4F) in these two models. Therefore, these findings suggest the potential for the broad application of targeting CCL5 for the treatment of acute liver injuries involving M2 macrophage-mediated liver resolution/repair, such as ALI and other acute liver diseases.

DISCUSSION

In the present study, we demonstrated the induction of CCL5 in drug-induced liver injury patients and an APAP-induced liver injury mouse model. We identified that multiple cell types, including hepatocytes and NPCs, are responsible for APAP-induced CCL5 expression. Functionally, we showed that CCL5 deficiency enhances liver repair in an ALI model by improving inflammation resolution and liver regeneration, which are mainly mediated by M2 macrophages. Mechanistically, we demonstrated that, through its receptors CCR1 and CCR5, CCL5 can facilitate M1 polarization and impede M2 polarization. Finally, we showed the therapeutic potential of inhibiting CCL5 in APAP overdose and suggested that targeting CCL5 may also play protective roles in other acute liver injuries induced by CCl₄ or IR.

Innate immunity activation and inflammatory surge are common features of various acute liver injuries. Generally, inflammation is believed to play a protective role through clearing cell debris and having proregenerative effects,³³ but unresolved inflammation serves as a detrimental factor in many liver diseases by aggravating liver damage.³⁴ Therefore, identifying the key factors that are able to regulate the switch between healthy and pathogenic inflammation is critical for developing novel therapeutic strategies against inflammation-related liver diseases. In fact, enhanced inflammation resolution has been reported to contribute to hepatic injury healing.^{24,35} Here we demonstrated a novel function of CCL5 as a key mediator of innate immunity regulation in acute liver injury.

In the early phase of APAP-induced liver injury, overdosed APAP is catalyzed by CYP2E1 to produce reactive NAPQI, which in turn forms cellular toxic protein adducts, especially mitochondrial protein adducts, leading to the dysfunction of mitochondria.² NAC, a GSH precursor, is the only approved treatment for neutralizing excessive NAPQI, but it is less effective in patients

whose liver injury has progressed to the late phase.⁷ In the present study, we demonstrated that CCL5 deficiency has no effect on detrimental early events, including APAP metabolism, GSH depletion, and mitochondrial dysfunction, but greatly improves inflammation resolution in the late phase of APAP-induced liver injury, suggesting that CCL5 may serve as a therapeutic target in the late phase of APAP overdose. This enhanced resolution seems to not be attributed to the reported chemotactic role of CCL5 on monocytes³⁶ because there was no difference in the number of hepatic macrophages in either WT or *Ccl5*^{-/-} mice. This may be explained by the fact that CCL5 is not the dominant chemokine responsible for monocyte trafficking during liver injury, given that previous studies have shown that hepatic monocyte recruitment in the liver occurs in a CCR2- or macrophage colony-stimulating factor-dependent manner.^{37,38} Although CCL5 has no effect on hepatic monocyte recruitment, we observed an increase in the number of M2 macrophages in *Ccl5*^{-/-} mice and that M2 macrophage depletion abolished the hepatoprotective role in *Ccl5*^{-/-} mice, suggesting that CCL5 may affect inflammation resolution by regulating macrophage polarization.

Polarization is a key feature of the remarkable plasticity of macrophages in response to various environmental stimuli.³⁹ M1 macrophages are known to be induced by TNF α , interferon- γ , and endotoxin, whereas M2 macrophages can be induced by IL-4, IL-10, and IL-13.⁴⁰ In addition to the cytokines that direct macrophage polarization, recent studies have demonstrated that some chemokine signals are also involved in macrophage polarization. For example, CX3CL1-CX3CR1 has been shown to suppress M1 polarization in microglia⁴¹; the inhibition of CXCL12-CXCR4 signaling significantly inhibits M1 polarization in adipose tissue.⁴² Here we identified CCL5-CCR1 and CCL5-CCR5 as alternative signaling pathways for modulating macrophage polarization. By interacting with downstream receptors, CCL5 activates intracellular MAPK and NF- κ B signaling pathways and promotes the M1 polarization of macrophages.

By employing a CCL5-neutralizing antibody (anti-CCL5) or a CCL5 antagonist (Met-CCL5), we evaluated the therapeutic potential of CCL5 signaling inhibition for the treatment of APAP overdose. To evaluate its therapeutic potential in the late phase, we first administered anti-CCL5 or Met-CCL5 24 h post-APAP injection, but no therapeutic effects were observed (data not shown), suggesting that the early inhibition of CCL5 signaling may be required to achieve desirable therapeutic effects despite the improved liver recovery in the late phase of APAP overdose in *Ccl5*^{-/-} mice. Following a two-injection strategy, we administered either anti-CCL5 or Met-CCL5 6 and 24 h after APAP treatment and found that CCL5 inhibition significantly ameliorated APAP-induced liver injury and improved survival. However, it is not reasonable to combine anti-CCL5 and Met-CCL5 to inhibit CCL5 because Met-CCL5 is a peptide antagonist that can also be neutralized by anti-CCL5. The combination of anti-CCL5 with an antagonist of CCL5 receptors may be feasible, but it was not examined in this study. In addition, given that acute liver injury induced either by CCl₄ or IR was ameliorated in *Ccl5*^{-/-} mice, it is worth investigating the therapeutic potential of CCL5 inhibition in these injury models.

MATERIALS AND METHODS

Patients and samples

Fifteen DILI patients were enrolled, and serum samples were collected. Ten of these patients underwent liver biopsy at the Department of Liver Diseases, Shuguang Hospital affiliated with Shanghai University of Chinese Traditional Medicine and the Department of Liver Surgery, Renji Hospital affiliated with the School of Medicine, Shanghai Jiao Tong University. Fifteen subjects were healthy controls. Samples from the healthy controls were collected at Renji Hospital affiliated with the School of Medicine, Shanghai Jiao Tong University. Patient samples were

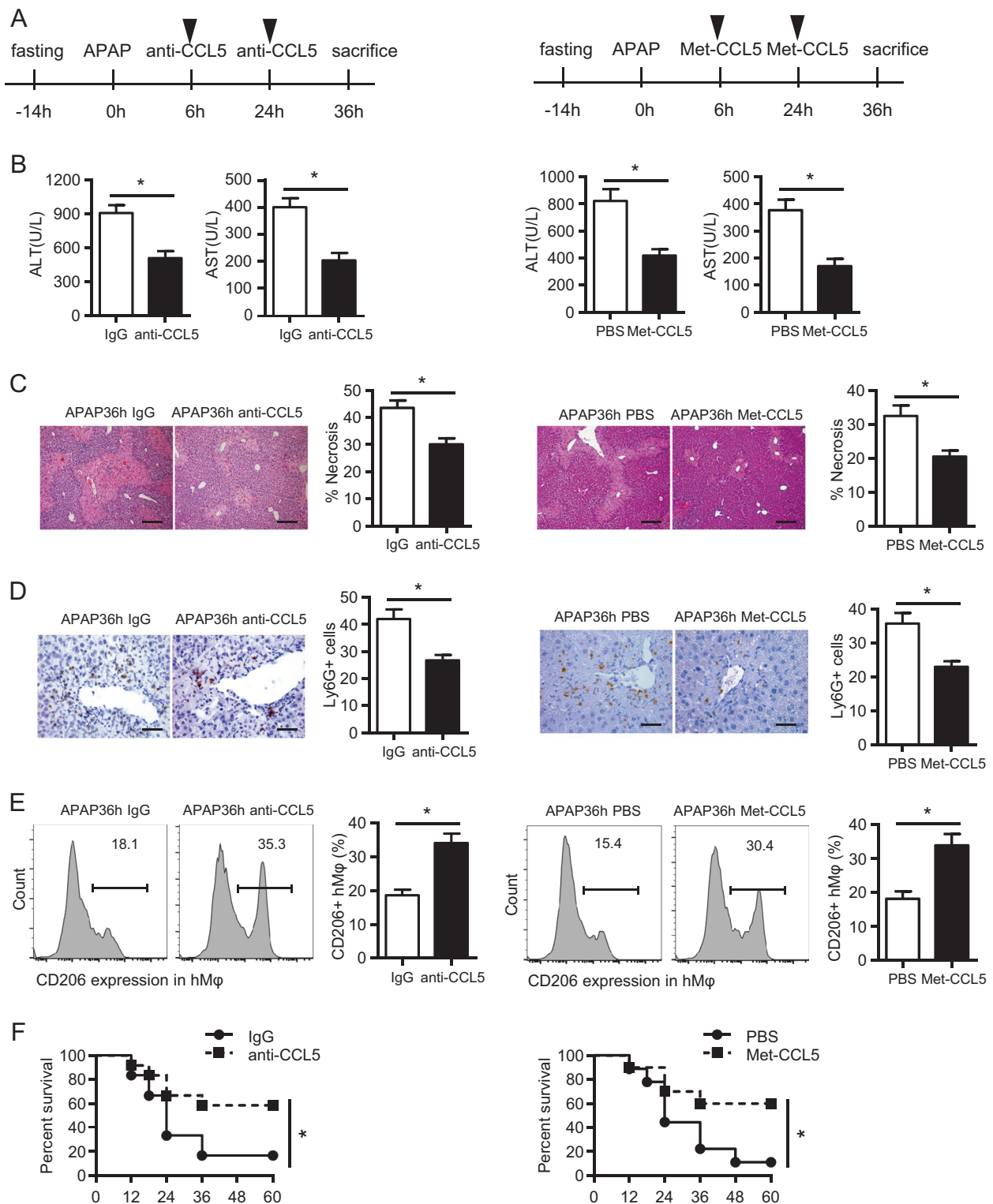


Fig. 7 CCL5 neutralization or inhibition facilitates liver recovery after acute liver injury. **a** A schematic of CCL5 inhibition by anti-CCL5 or Met-CCL5 in the APAP overdose model. The dose of anti-CCL5 and Met-CCL5 was 10 μ g. **b** Serum levels of ALT/AST were detected after anti-CCL5- or Met-CCL5-mediated CCL5 blockage ($n = 4-6$). **c** Representative images of H&E staining (original magnification = $\times 100$, scale bar = 200 μ m) and the statistical quantification of hepatic necrosis upon anti-CCL5- or Met-CCL5-mediated CCL5 inhibition ($n = 4-6$). **d** Representative images and the statistical quantification of hepatic Ly6G⁺ cells in liver sections (original magnification = $\times 400$, scale bar = 50 μ m) upon anti-CCL5- or Met-CCL5-mediated CCL5 inhibition ($n = 4-6$). **e** Representative FACS plots and the statistical quantification of CD206⁺ hepatic macrophages (hM ϕ) upon anti-CCL5- or Met-CCL5-mediated CCL5 inhibition ($n = 4-6$). **f** Survival curves of mice ($n = 10-12$) in response to a lethal dose of APAP treatment upon anti-CCL5- or Met-CCL5-mediated CCL5 inhibition. The data are shown as means \pm SEM, * $P < 0.05$

obtained following informed consent and according to protocols approved by the ethical review committees of Shanghai University of Chinese Traditional Medicine and Shanghai Jiao Tong University. To analyze CCL5 expression at the protein level, serum CCL5 expression was analyzed using an ELISA kit, and tissue CCL5 expression was analyzed using IHC. The patients' clinical information is shown in Supplementary Table 1.

Animal and animal models

Ccl5 knockout (*Ccl5*^{-/-}, B6.129P2-*Ccl5*^{tm1Hso}/J, stock no: 005090) mice were purchased from the Jackson Laboratory (Bar Harbor, ME). The APAP liver injury model was established as in our previous study.²³ Briefly, 20 mg/ml APAP solution was freshly prepared by dissolving APAP (Sigma-Aldrich, St. Louis, MO) in pyrogen-free phosphate-buffered saline (PBS) at 55 °C. Then freshly prepared APAP solution was warmed to 37 °C and injected i.p. at a dose of 300 mg/kg (sublethal dose) or 500 mg/kg (lethal dose) into mice that had been fasted overnight. To evaluate the therapeutic potential of CCL5 inhibition, a CCL5-neutralizing antibody (anti-CCL5, AF478, R&D, USA); control IgG (AB-108-C, R&D, USA); or a CCL5 receptor antagonist (Met-CCL5, 335-RM/CF, R&D, USA) were reconstituted in sterile PBS and administered to WT mice (10 µg/injection, i.p) 6 and 24 h after APAP overdose. Liver tissues and serum samples were collected at the indicated time points. For all in vivo experiments, we used age-matched (8–10-week-old) male *Ccl5*^{-/-} mice and WT littermate controls bred in specific pathogen-free conditions. The littermates were offspring that were generated from heterozygous mice (*Ccl5*^{+/-}). All mouse studies were approved by the Institutional Animal Care and Use Committees of Renji Hospital and Shanghai Jiao Tong University.

Statistical analysis

GraphPad Prism 6 software (GraphPad Software, San Diego, CA, USA) was used for statistical analysis. The results are presented as means ± SEM unless otherwise stated. Comparisons of two groups were performed using paired or unpaired Student's *t* test. Survival curves were compared using log-rank (Mantel–Cox) test.

Other methods are included in Supplementary Materials And Methods.

ACKNOWLEDGEMENTS

We thank Dr. Zhang Yan at Shanghai Jiao Tong University for providing *Ccl5*^{-/-} mice. This work was supported by the National Key Research and Development Program of China (2017YFC0908100 to Q.X.), the National Key Sci-Tech Special Project of China (2018ZX10723204-006-004 to X.K.), the National Natural Science Foundation of China (81873582 and 81670562 to X.K., 81670598 to Q.X., 31870905 and 31671453 to H.W.), and the Shanghai Municipal Education Commission—Gaofeng Clinical Medicine Grant Support (20171911 to X.K.).

AUTHOR CONTRIBUTIONS

M.L. performed the experiments and wrote the manuscript. X.S., R.L., and Q.X. made the clinical diagnoses and collected the clinical samples. L.X., J.L., M.X., B.W., H.G., C.Y., J.Z., and Y.G. contributed to data collection and performed some experiments. H.W. critically edited the manuscript. X.K. and Q.X. designed and supervised the project and revised the manuscript for important content.

ADDITIONAL INFORMATION

The online version of this article (<https://doi.org/10.1038/s41423-019-0279-0>) contains supplementary material.

Competing interests: The authors declare no competing interests.

REFERENCES

- Lee, W. M. Drug-induced acute liver failure. *Clin. Liver Dis.* **17**, 575–586 (2013).

- Jaeschke, H., Williams, C. D., Ramachandran, A. & Bajt, M. L. Acetaminophen hepatotoxicity and repair: the role of sterile inflammation and innate immunity. *Liver Int.* **32**, 8–20 (2012).
- Dahlin, D. C., Miwa, G. T., Lu, A. Y. & Nelson, S. D. N-acetyl-p-benzoquinone imine: a cytochrome P-450-mediated oxidation product of acetaminophen. *Proc. Natl Acad. Sci. USA* **81**, 1327–1331 (1984).
- Jaeschke, H., Duan, L., Akakpo, J. Y., Farhood, A. & Ramachandran, A. The role of apoptosis in acetaminophen hepatotoxicity. *Food Chem. Toxicol.* **118**, 709–718 (2018).
- Tran, T. & Lee, W. M. DILI: New Insights into Diagnosis and Management. *Curr. Hepat. Rep.* **12**, (53–58 (2013).
- Saito, C., Zwingmann, C. & Jaeschke, H. Novel mechanisms of protection against acetaminophen hepatotoxicity in mice by glutathione and N-acetylcysteine. *Hepatology* **51**, 246–254 (2010).
- Barbier-Torres, L. et al. The mitochondrial negative regulator MCJ is a therapeutic target for acetaminophen-induced liver injury. *Nat. Commun.* **8**, 2068 (2017).
- Zhang, C. et al. Macrophage-derived IL-1α promotes sterile inflammation in a mouse model of acetaminophen hepatotoxicity. *Cell. Mol. Immunol.* **15**, 973–982 (2018).
- Jaeschke, H. Mechanisms of sterile inflammation in acetaminophen hepatotoxicity. *Cell. Mol. Immunol.* **15**, 74–75 (2018).
- Epelman, S., Lavine, K. J. & Randolph, G. J. Origin and functions of tissue macrophages. *Immunity* **41**, 21–35 (2014).
- Sica, A., Erreni, M., Allavena, P. & Porta, C. Macrophage polarization in pathology. *Cell. Mol. Life Sci.* **72**, 4111–4126 (2015).
- Adams, D. H., Ju, C., Ramaiah, S. K., Uetrecht, J. & Jaeschke, H. Mechanisms of immune-mediated liver injury. *Toxicol. Sci.* **115**, 307–321 (2010).
- Marra, F. & Tacke, F. Roles for chemokines in liver disease. *Gastroenterology* **147**, 577–594 e571 (2014).
- Long, H. et al. Autocrine CCL5 signaling promotes invasion and migration of CD133+ ovarian cancer stem-like cells via NF-κB-mediated MMP-9 upregulation. *Stem Cells* **30**, 2309–2319 (2012).
- Wang, S. W. et al. CCL5 and CCR5 interaction promotes cell motility in human osteosarcoma. *PLoS ONE* **7**, e35101 (2012).
- Kim, J. E. et al. LYR71, a derivative of trimeric resveratrol, inhibits tumorigenesis by blocking STAT3-mediated matrix metalloproteinase 9 expression. *Exp. Mol. Med.* **40**, 514–522 (2008).
- Marques, R. E., Guabiraba, R., Russo, R. C. & Teixeira, M. M. Targeting CCL5 in inflammation. *Expert Opin. Ther. Targets* **17**, 1439–1460 (2013).
- Li, B. H., He, F. P., Yang, X., Chen, Y. W. & Fan, J. G. Steatosis induced CCL5 contributes to early-stage liver fibrosis in nonalcoholic fatty liver disease progress. *Transl. Res.* **180**, 103–117 e104 (2017).
- Berres, M. L. et al. Antagonism of the chemokine Ccl5 ameliorates experimental liver fibrosis in mice. *J. Clin. Invest* **120**, 4129–4140 (2010).
- Sadeghi, M. et al. Serum levels of chemokines CCL4 and CCL5 in cirrhotic patients indicate the presence of hepatocellular carcinoma. *Br. J. Cancer* **113**, 756–762 (2015).
- Mohs, A. et al. Functional role of CCL5/RANTES for HCC progression during chronic liver disease. *J. Hepatol.* **66**, 743–753 (2017).
- Lee, C. M. et al. C-C chemokine ligand-5 is critical for facilitating macrophage infiltration in the early phase of liver ischemia/reperfusion injury. *Sci. Rep.* **7**, 3698 (2017).
- Wen, Y. et al. Metabolic modulation of acetaminophen-induced hepatotoxicity by osteopontin. *Cell. Mol. Immunol.* **16**, 483–494 (2018).
- Triantafyllou, E. et al. MerTK expressing hepatic macrophages promote the resolution of inflammation in acute liver failure. *Gut* **67**, 333–347 (2018).
- Bird, T. G. et al. TGFβ inhibition restores a regenerative response in acute liver injury by suppressing paracrine senescence. *Sci. Transl. Med.* **10**, eaan1230 (2018).
- Bhushan, B. & Apte, U. Liver regeneration after acetaminophen hepatotoxicity: mechanisms and therapeutic opportunities. *Am. J. Pathol.* **189**, 719–729 (2019).
- Laskin, D. L. Macrophages and inflammatory mediators in chemical toxicity: a battle of forces. *Chem. Res Toxicol.* **22**, 1376–1385 (2009).
- Choi, K. M. et al. CD206-positive M2 macrophages that express heme oxygenase-1 protect against diabetic gastroparesis in mice. *Gastroenterology* **138**, 2399–2409 (2010). 2409 e2391.
- Zhou, D. et al. Macrophage polarization and function with emphasis on the evolving roles of coordinated regulation of cellular signaling pathways. *Cell. Signal.* **26**, 192–197 (2014).
- Lawrence, T. & Natoli, G. Transcriptional regulation of macrophage polarization: enabling diversity with identity. *Nat. Rev. Immunol.* **11**, 750–761 (2011).
- Shi, J., Aisaki, K., Ikawa, Y. & Wake, K. Evidence of hepatocyte apoptosis in rat liver after the administration of carbon tetrachloride. *Am. J. Pathol.* **153**, 515–525 (1998).
- Ren, F. et al. Inhibition of glycogen synthase kinase 3β ameliorates liver ischemia reperfusion injury by way of an interleukin-10-mediated immune regulatory mechanism. *Hepatology* **54**, 687–696 (2011).

33. Woolbright, B. L. & Jaeschke, H. Sterile inflammation in acute liver injury: myth or mystery? *Expert Rev. Gastroenterol. Hepatol.* **9**, 1027–1029 (2015).
34. Perugorria, M. J. et al. Non-parenchymal TREM-2 protects the liver from immune-mediated hepatocellular damage. *Gut* <https://doi.org/10.1136/gutjnl-2017-314107> 2018.
35. Liew, P. X., Lee, W. Y. & Kubes, P. iNKT cells orchestrate a switch from inflammation to resolution of sterile liver injury. *Immunity* **47**, 752–765 e755 (2017).
36. von Hundelshausen, P. et al. Heterophilic interactions of platelet factor 4 and RANTES promote monocyte arrest on endothelium. *Blood* **105**, 924–930 (2005).
37. Mossanen, J. C. et al. Chemokine (C-C motif) receptor 2-positive monocytes aggravate the early phase of acetaminophen-induced acute liver injury. *Hepatology* **64**, 1667–1682 (2016).
38. Stutchfield, B. M. et al. CSF1 restores innate immunity after liver injury in mice and serum levels indicate outcomes of patients with acute liver failure. *Gastroenterology* **149**, 1896–1909 e1814 (2015).
39. Mantovani, A., Sozzani, S., Locati, M., Allavena, P. & Sica, A. Macrophage polarization: tumor-associated macrophages as a paradigm for polarized M2 mononuclear phagocytes. *Trends Immunol.* **23**, 549–555 (2002).
40. Ruytinx, P., Proost, P., Van Damme, J. & Struyf, S. Chemokine-induced macrophage polarization in inflammatory conditions. *Front Immunol.* **9**, 1930 (2018).
41. Mattison, H. A. et al. Suppressed pro-inflammatory response of microglia in CX3CR1 knockout mice. *J. Neuroimmunol.* **257**, 110–115 (2013).
42. Kim, D. et al. CXCL12 secreted from adipose tissue recruits macrophages and induces insulin resistance in mice. *Diabetologia* **57**, 1456–1465 (2014).